Asian Journal of Chemistry; Vol. 34, No. 9 (2022), 2311-2317

ASIAN JOURNAL OF CHEMISTRY

https://doi.org/10.14233/ajchem.2022.23815

Molecular Docking Studies and *in silico* ADMET Screening of Indazole Scaffolds as VEGFR and Enoyl-ACP (CoA) Reductase Inhibitors

ANURUDDHA R. CHABUKSWAR[1,*], RAJESH B. NANAWARE[1], SWATI JAGDALE[2], SURAJ B. NANAWARE[3] and JAIPRAKASH SANGSHETTI[4]

[1]Department of Pharmaceutical Chemistry, School of Pharmacy, Dr. Vishwanath Karad MIT World Peace University, Pune-411038, India
[2]Department of Pharmaceutics, School of Pharmacy, Dr. Vishwanath Karad MIT World Peace University, Pune-411038, India
[3]Department of Pharmaceutics, Shri Bhairavnath Nisarg Mandals College of Pharmacy, Osmanabad-413501, India
[4]Department of Pharmaceutical Chemistry, Y.B. Chavan College of Pharmacy, Aurangabad-431001, India

*Corresponding author: E-mail: anuruddha.chabukswar@mitwpu.edu.in

Received: 3 March 2022; *Accepted*: 16 June 2022; *Published online*: 19 August 2022; AJC-20927

Lung cancer is expected to account for 11.4 % of the cancer burden in 2020, with an estimated 2.2 million new cases diagnosed and 1.8 million deaths occurring. Non-small-cell lung cancer accounted for approximately 85% of newly diagnosed lung cancer cases. In non-small cell lung cancer and tuberculosis level of vascular endothelial growth factor was found to be elevated, which induces angiogenesis. In this study molecular docking analysis along with pharmacokinetic/ADMET and drug likeness prediction were carried out to evaluate the newly designed indazole scaffolds as potent VEGFR and Enoyl-ACP (CoA) reductase enzyme inhibitors. Out of 11 screened compounds, two compounds having good scores (-7.72 and -7.54 kcal/mol) emerged as effective and potent VEGFR-2 inhibitors and three compounds showed highest binding affinities (-8.30, -7.76, -7.62 kcal/mol) with Enoyl-ACP. This study reveals that, newly designed indazole compounds could be the potential drug of choice against non-small cell lung cancer and tuberculosis.

Keywords: Lung cancer, ADMET, Enoyl-ACP reductase, Indazole, Molecular Docking, VEGFR.

INTRODUCTION

After breast cancer, lung cancer is the second most commonly diagnosed cancer worldwide, and its prevalence is continuously increasing. Lung cancer is expected to account for 11.4% cancer burden in 2020, with an estimated 2.2 million new cases diagnosed. An estimated 18% (1.8 million) lung cancer death occurred in 2020 [1]. Non-small cell lung cancer (NSCLC) accounted for approximately 85% of newly diagnosed lung cancer cases [2]. Angiogenesis is known to be stimulated by abnormal activation of vascular endothelial growth factor receptors (VEGFRs), which causes cell proliferation, migration, survival, and permeability of blood vessels [3,4]. Since discovering the critical functions of RTKs (receptor tyrosine kinases) in tumor development and progression in the last few decades, inhibiting RTKs to prevent cancer growth and metastasis has become a promising method for developing new anticancer drugs [5,6]. Several VEGFR inhibitors, including indol-based sunitinib, nintedanib, indazole-based pazopanib and axitinib, urea derivative sorafenib and lavatinib, have been approved for cancer treatment therapy [7,8]. The level of VEGF in tuberculosis (TB) patients is raised, according to *in vitro* and *in vivo* studies. In active pulmonary tuberculosis lesions, intense angiogenesis has been seen [9,10]. VEGF levels were thus elevated in both NSCLC and tuberculosis. However, the efficacy of these anti-angiogenic drugs has been impaired by resistance and severe side effects, suggesting that VEGFR domain could be a promising target for the development of novel anticancer treatments in NSCLC. In 2019, an estimated 10.0 million individuals worldwide developed tuberculosis. Drug-resistant tuberculosis continues to be a public health threat. In 2019, nearly half a million persons got rifampicin-resistant tuberculosis (RR-TB), with 78% having multidrug-resistant tuberculosis (MDR-TB). In 2019, tuberculosis claimed the lives of 1.4 million individuals, including 2,08000 HIV-positive people [11]. The indazole scaffold has been studied extensively for the development of newer pharmaceutical drugs and numerous indazole derivatives exhibit their capacity to inhibit VEGFR-2 and mycobacterium tuberculosis [12-14].

Anti-angiogenic medicines, when used in conjunction with anti-tuberculosis medications, have the potential to increase antimicrobial drug delivery into aberrant vasculature and stimulate sensitivity to drug therapy *via* oxygen during the window of normalization [15]. Hence in this context, present research focuses on the computational design of novel VEGFR-2 and Enoyl-ACP (CoA) reductase enzyme (InhA) inhibitors with better inhibitory effects by using docking studies and ADMET prediction.

EXPERIMENTAL

This computational work was carried out on a computer with an Intel Core i5-4570 CPU operating at 3.20 GHz and 4GB of RAM. Softwares such as Autodock 4.2.6, UCSF Chimera 1.15, ACD/ChemSketch (Freeware-drawing package), Biovia discovery studio visualizer, Open Babel GUI 3.1.1, an open chemical toolbox for molecular docking and Swiss ADME: a free web tool for ADME prediction, were used.

Ligand preparation: Using the ACD/ChemSketch software, a set of eleven newly designed compounds with an indazole scaffold was created. All the 3D structures were converted into PDB file format utilizing Open Babel GUI [16] and then the energy of all the structures were minimized by assigning 100 steps of steepest descent and 10 steps of conjugate gradient energy minimization in UCSF-Chimera software [17]. All the energy minimized structures were converted into PDBQT file format after detecting root, number of torsions and aromaticity criteria (≤ 7.5) with the help of Autodock tools [18,19]. Two dimensional structures of designed ligands are represented in Table-1.

Receptor preparation: The 3D crystal structure of VEGFR-2 (PDB ID: 4AGD) and Enoyl-ACP (CoA) reductase enzyme (InhA) (PDB ID: 2AQK) were retrieved from the protein data bank [20,21]. Water molecules, ions and other ligands present in the protein were removed and the polar hydrogens and Kollman charges were added to the proteins. The PDB format files of proteins were converted into PDBQT file format after assigning AD4 charges. The grid parameter (.gpf) files were prepared by adjusting the size dimension of grid box as 40 × 40 × 50 and 98 × 98 × 98 (0.5 Å spacing) for both 4AGD and 2AQK proteins respectively. After, the grid log files (.glg) were prepared by launching Autogrid. By utilizing docking parameter file (.dpf), docking log file (.dlg) were generated using ADT. The docking study was performed by using genetic search Lamarkain algorithm to explore the best conformational space for the ligand with 10 docking runs for each ligand. The maximum number of generations and evaluation were set at 27000 and 2500000, respectively. Finally the best-fit comp-

TABLE-1
STRUCTURES OF NEWLY DESIGNED COMPOUNDS AGAINST NON-SMALL CELL LUNG CANCER AND TUBERCULOSIS

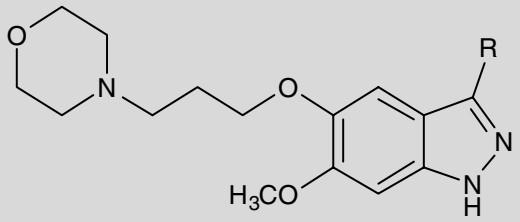

S. No.	Compd. code	R	S. No.	Compd. code	R
1	ACF	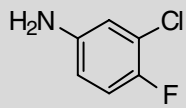	7	ADM	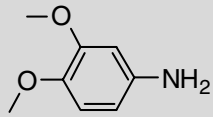
2	ACN	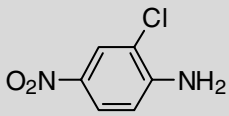	8	AF	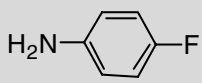
3	AA	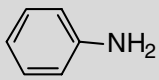	9	AI	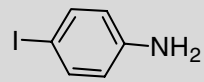
4	AC	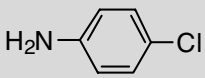	10	AN	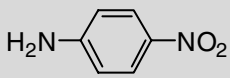
5	ADC	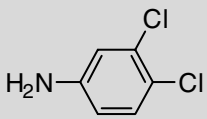	11	ATM	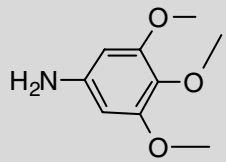
6	ADF	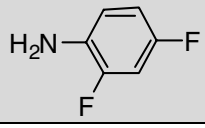	–	–	–

lexes were analyzed manually using ADT. The docked receptor and ligands interactions were visualized and ranked based on binding energy using discovery studio visualizer.

Drug-likeness and ADMET properties prediction: In this present study, a free online web tool of SwissADME was used to predict the Lipinski's parameters, pharmacokinetic properties, synthetic accessibility and toxicity of compounds [22-25]. The bioavailability and transportation of an effective compound across the blood-brain barrier were predicted using topological polar surface area (tPSA) [26]. In some of the earlier studies, docking interactions of indzaole showed potential as antibacterial agent [27].

RESULTS AND DISCUSSION

Molecular docking studies of designed compounds: All the newly designed indazole based inhibitors showed negative binding energy.

Binding profile of newly designed inhibitors against 4AGD: Out of 11 compounds screened against 4AGD some of the compounds showed significant binding energies when compared with standard ligands. Compounds showing significant interactions are as follows:

Compound AA showed the highest binding energy value of -7.72 kcal/mol and formed three hydrogen bonds with LEU840, ASN923, ARG842 amino acid residues and bond distances were 2.09, 2.17 and 2.17 Å, respectively. Followed by compound AF showed binding energy value of -7. 54 kcal/mol and two hydrogen bond interactions were observed with amino acid positions ARG1032 and ASN923 and their bond distances were 2.25 and 2.57 Å, respectively. Besides hydrogen bonds, it formed halogen bond with ASP1058 amino acid and π-π bond with PHE1047. Compound AI showed the binding energy value of -5.65 kcal/mol, formed 3-hydrogen bond interactions with amino acids ILE1111, ARG1061 and PRO1057 (bond distances 2.24, 2.35 and 2.80 Å, respectively). It also formed carbon-hydrogen bond with amino acid THR1059 and PRO1057, π-σ bond with VAL1060 amino acid. Compound ACF showed the binding energy of -5.65 kcal/mol, formed one hydrogen bond interaction with amino acid SER1154 (2.48 Å). It also formed carbon hydrogen bonds with ASP807 and ALA1020 and alkyl bond with amino acid ILE1084. Compound ADC showed binding energy value of -5.57 kcal/mol and formed 2 hydrogen bonds with amino acid GLU1048 and SER803 residues with distance 2.16 and 2.27 Å. It also formed carbon hydrogen bonds with amino acid ARG1051, ARG1066 and other hydrophobic bonds with PRO1068, LEU1067, ALA844 and TYR1054 (Table-2). Fig. 1 represent the docking score and amino acids involved in hydrophobic interactions of newly designed compounds against 4AGD.

Binding profile of newly designed inhibitors against 2AQK: All 11 newly designed compounds were screened against 2AQK. Compound ADC has the highest binding affinity of -8.30 kcal/mol, formed 3 hydrogen bonds with GLY96, ILE194 and GLY14 (bond distances 2.01, 2.18 and 2.36 Å, respectively) amino acid residues. It forms hydrophobic bonds with MET199, MET147, ILE21, ALA94, VAL65, ILE95 and PHE41. The second best designed compound ACN has binding affinity of -7.76 kcal/mol and formed three hydrogen bonds with GLY14 (2.10 Å), MET98 (2.12 Å) and THR (2.23 Å) amino acid residues. It also forms carbon-hydrogen bond with GLY96 (4.78 Å) amino acid and other hydrophobic bonds with PHE97, PHE41, ALA198, ILE122, ILE16 and ILE95 amino acid residues. Compound AI showed binding energy value of -7.62 kcal/mol and it formed one hydrogen bond with MET98 (2.14 Å). It also formed carbon hydrogen bond with GLY96 and other interactions with MET161, MET147, ILE21, ILE 95, ILE122, ALA94, ALA22, PHE41 and PHE97 amino acid residues. Compound ADF has binding energy of -7.35 kcal/mol and formed two hydrogen bonds with ILE194 (1.84Å) and GLY14 (1.96Å). It also formed carbon hydrogen bonds with ASP148 & ILE95 and halogen bonds with ALA94 and GLY96. In addition it forms hydrophobic bonds with ALA94, MET194, MET147, ILE21, PHE149 and ALA22. Compound ACF has binding affinity of -7.33 kcal/mol and formed two hydrogen bonds with amino acid GLY96 (1.68 Å) and GLY14 (2.22 Å). It forms hydrophobic bonds with ILE122, ILE21 PHE41, GLU810, ILE95, ALA194 and MET199 amino acid residues (Table-3). Fig. 2 indicates the docking score and

TABLE-2
TYPES OF INTERACTIONS OF NEWLY DESIGNED VEGFR-2 INHIBITORS WITH 4AGD

Entry	Binding affinities (kcal/mol)	Conventional hydrogen bond	Bond angle (Å)	Hydrophobic and other interactions
ACF	-5.65	SER1154	2.48	ASP807, ALA1020, ILE1084
ACN	-5.27	LYS1070, ARG1061	2.41, 2.55	ASP1058, PRO1057, VAL1060, ILE1111
AA	-7.72	LEU840, ASN923, ARG842	2.09, 2.17, 2.17	ASP1058, ASN923, ARG1032, ARG1051, PHE1047
AC	-5.15	LEU840, SER930	2.93, 2.23	ALA866, VAL916, VAL848, CYS919, PHE918
ADC	-5.57	GLY1048, SER803	2.16, 2.27	ARG1066, ARG1051, TYR1054, ALA844, PRO1068, LEU1067
ADF	-5.55	CYS919	2.93	LYS868, LEU840, VAL848, VAL916, LEU1035, CYS1045, ALA866, PHE918
ADM	-3.93	–	–	GLU1146, ASP809, GLU1075, PRO1147, LYS1023, ALA1020, VAL1081
AF	-7.54	ARG1032, ASN923	2.25, 2.57	ASP1058, PHE1047
AI	-5.65	ILE1111, ARG1061, PRO1057	2.24, 2.35, 2.80	TYR1059, VAL1060
AN	-4.82	CYS919	2.06	LYS868, PRO839, LEU840, LEU1035, VAL848, ALA868, PHE918
ATM	-4.62	TYR1082	2.63	GLU810, ASP809, PRO808, ALA1020, LYS1023, ILE1084

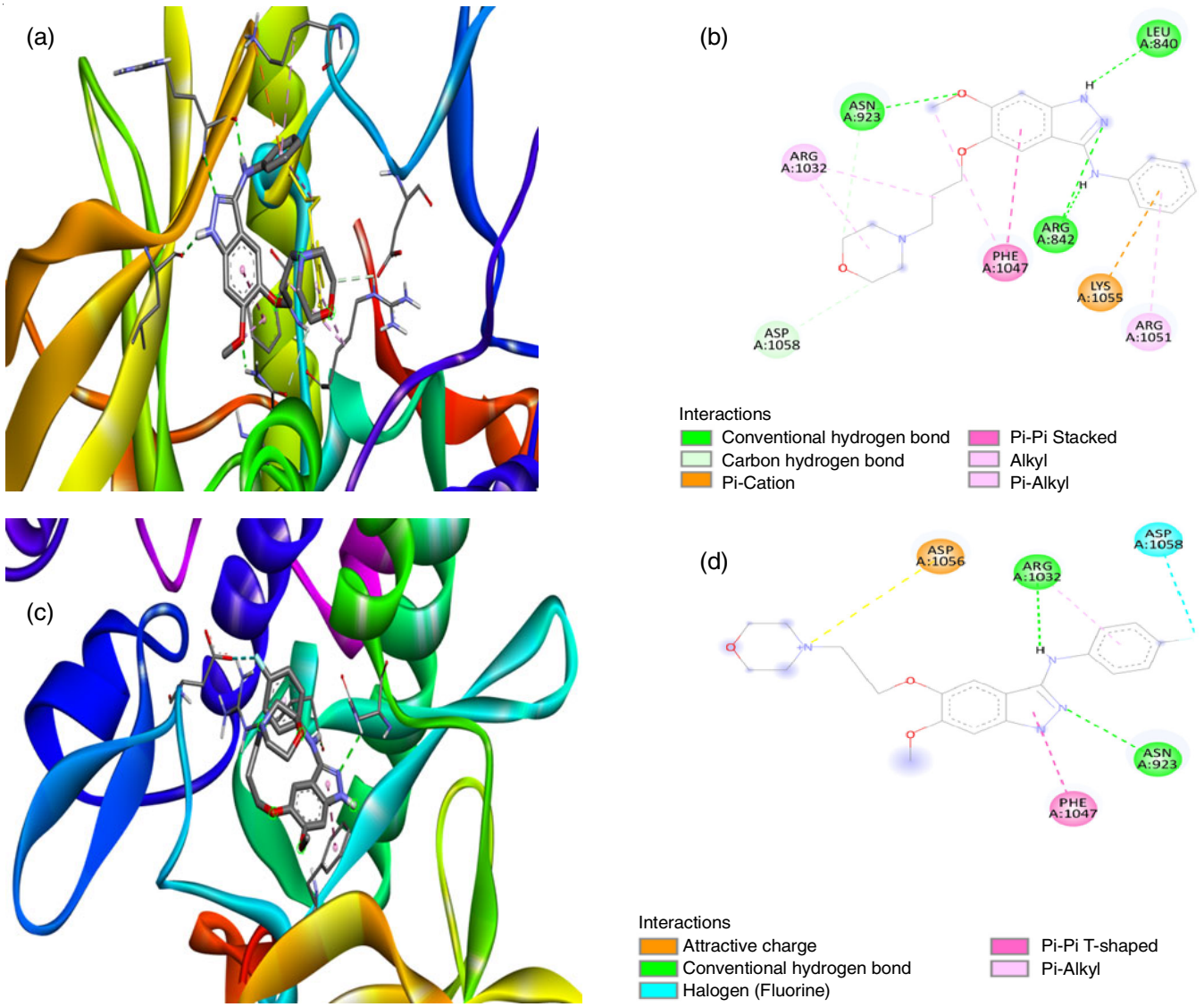

Fig. 1. (a) Docked complex of AA, (b) 2D interaction diagram of AA with 4AGD, (c) docked complex of AF, (d) 2D interaction diagram of AF with 4AGD

TABLE-3
TYPES OF INTERACTIONS OF NEWLY DESIGNED TUBERCULOSIS INHIBITORS WITH 2AQK

Entry	Binding affinities	Conventional hydrogen bonds	Bond angle (Å)	Hydrophobic and other interactions
ACF	-7.33	GLY96, GLY14	1.68, 2.22	GLU810, ILE95, 194, & 21, MET199, ILE122, ALA94, PHE41, ASP809
ACN	7.76	GLY14, MET98, THR39	2.10, 2.12, 2.23	PHE97, ALA198, ILE16, ILE122, ILE95, GLY96, PHE41.
AA	-7.25	LYS165	2.20	MET161, ILE94, ILE195, ASP148, ALA191, 94 &22, ILE21, MET147
AC	-7.15	ILE194, GLY14, GLY96	1.84, 2.13, 2.35	ILE21, MET199, ILE95, ILE122, PHE41, VAL65
ADC	-8.30	GLY96, ILE194, GLY14	2.01, 2.18, 2.36	MET147, ILE21, MET199, ALA94, ILE95, VAL65, PHE41
ADF	-7.35	ILE194, GLY14	1.84, 1.96	PHE149, MET199, GLY96, ILE95, ALA22 &94, ASP148, ILE21, MET147
ADM	-6.13	GLY14	2.33	ASP148, MET147, MET161, ALA94, ALA22, ILE21, 95 &122, GLY96
AF	-7.09	ILE194, GLY96	1.80, 2.22	ALA22, 94 & 191, ILE21, GLY14, SER20, MET147&161, TYR158, PHE149
AI	-7.62	MET98	2.14	MET161, MET147, ILE21, 95 & 122, ALA22 & 94, PHE41, PHE97, GLY96
AN	-7.01	SER20, ASP148, MET98	1.97, 2.13, 2.14	GLY96, PRO193, PHE97 &149, ALA191, MET147, 161&199, TYR158, ILE21
ATM	-6.13	PHE108, ALA157, MET155	2.18, 2.19. 2.30	VAL163, ALA154, PRO107, ILE105, GLY104, GLN214, PRO156

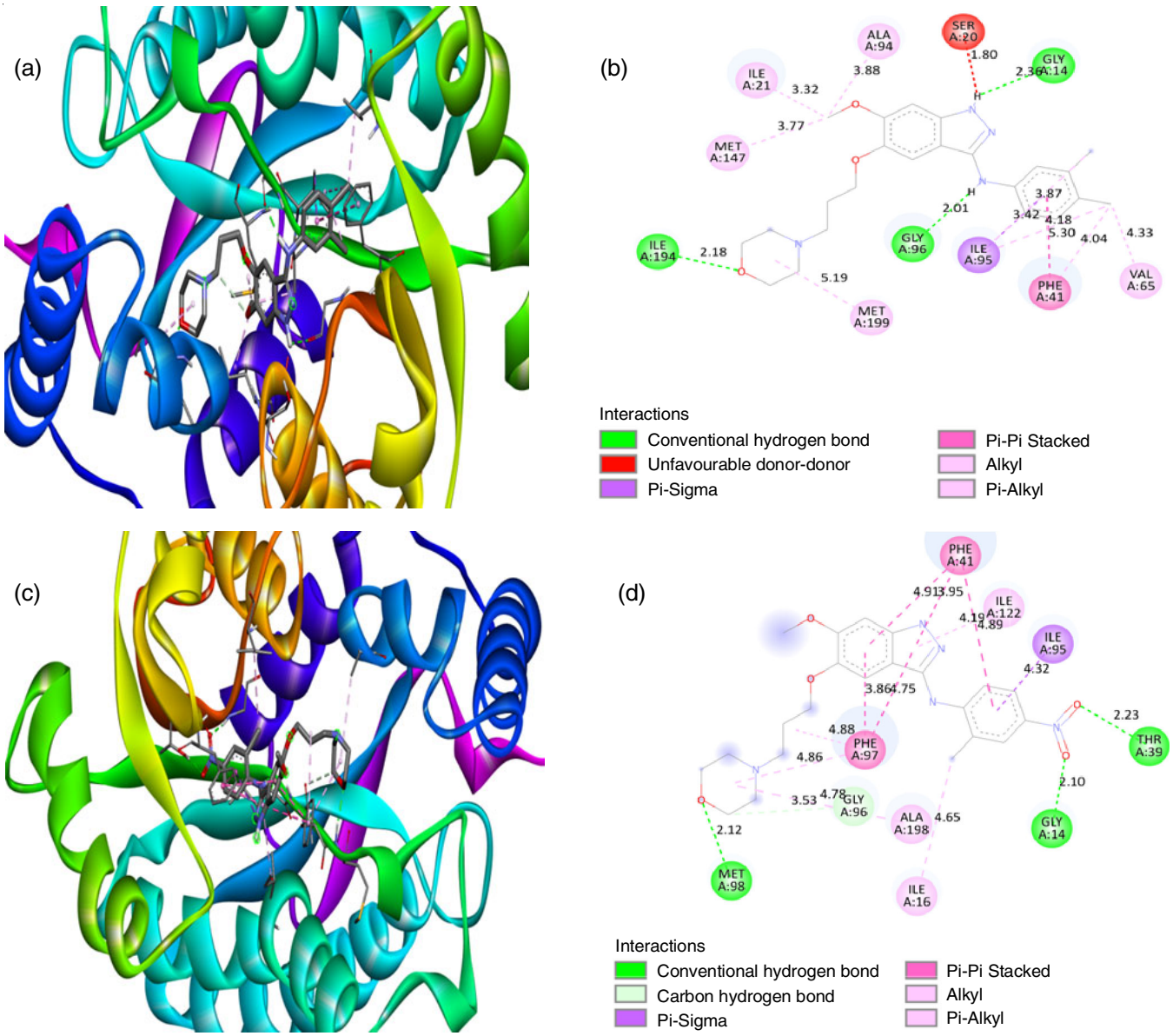

Fig. 2. (a) Docked complex of ADC, (b) 2D interaction diagram of ADC with 2AQK, (c) docked complex of ACN, (d) 2D interaction diagram of ACN with 2AQK

amino acid involved in hydrophobic interactions of newly designed compounds against 2AQK. Docking calculations were validated by redocking ligand that was co-crystallized in the receptor structure of 4AGD and docking standard isoniazid with 2AQK. In case of receptor 4AGD, most of the indazole based compounds display significant docking score as compared to the standard drug sunitinib which has the binding energy -9.10 kcal/mol. When it came to 2AQK, all of the newly designed indazole based compounds surpassed the standard drug isoniazid, which has a binding energy of -5.26 kcal/mol.

Drug-likeness and ADME properties prediction: The drug-likeness properties of the designed compounds were predicted following Lipinski's Rule of Five. All the tested compound passes Lipinski's Rule of Five with 0 violation except compound-3 (AI) passes with one violation MW > 500 and compound-11 (ADM) passes with one violation rotatable bonds >10. The number of hydrogen bond donors and acceptors for all was less than 5 and 10, respectively. The passive molecular transport over membranes as well as the blood-brain barrier was correlated with the property topological polar surface are (tPSA).The molecules having tPSA value < 140 Å^2 passes the standard for GI absorption. In contrast, all tested compounds except compound 7 and 9 (tPSA 117.46Å2) and compound-10 (tPSA 99.33 Å^2) have a low BBB penetration (tPSA > 90.00 Å^2), that indicates the side effects of CNS are compact or inattentive but not in case of other compounds. All the tested compounds were found to have WLOGp values (which predicts whether a molecule has low toxicity level or not) less than 5. The synthetic accessibility score of these newly designed compounds on the scale were in the easy portion (< 5). It means these compounds can be easily synthesizable in the laboratory (Table-4). Bioavailability of the tested compounds was found to be 0.55. On that basis, the newly designed compounds predicted to be drug-like compounds, orally bioavailable and active.

TABLE-4
DRUG-LIKENESS PROPERTIES OF THE NEWLY DESIGNED COMPOUNDS

Compd. code	MW	tPSA	WLOGP	HBD	HBA	RO5 violation	RB	SA
ACF	434.89	71.64	4.25	2	6	0	8	3.29
ACN	461.90	117.46	3.60	2	7	0	9	3.47
AA	382.46	71.64	2.19	2	5	0	8	3.19
AC	416.90	71.64	3.69	2	5	0	8	3.20
ADC	451.34	71.64	4.34	2	5	0	8	3.27
ADF	418.44	71.64	4.15	2	7	0	8	3.34
ADM	442.51	90.10	1.32	2	7	0	10	3.56
AF	400.45	71.64	3.69	2	6	0	8	3.21
AI	508.35	71.64	2.89	2	5	1	8	3.39
AN	427.45	117.46	2.94	2	7	0	9	3.37
ATM	472.53	99.33	3.06	2	8	0	11	3.74

MW: molecular weight; tPSA: total polar surface area; HBD: hydrogen bond donars; HBA: hydrogen bond acceptors; RB: rotatable bonds; SA: synthetic accessibility.

TABLE-5
ADME PROPERTIES OF NEWLY DESIGNED COMPOUNDS

Compd. code	GI absorption	BBB permeant	Pgp substrate	Bioavil-ability score	CYP1 A2 inhibitor	CYP2 C19 inhibitor	CYP2 C9 inhibitor	CYP2 D6 inhibitor
ACF	High	Yes	Yes	0.55	Yes	Yes	Yes	Yes
ACN	High	No	No	0.55	No	Yes	Yes	Yes
AA	High	Yes	Yes	0.55	Yes	Yes	Yes	Yes
AC	High	Yes	Yes	0.55	Yes	Yes	Yes	Yes
ADC	High	Yes	No	0.55	No	Yes	Yes	Yes
ADF	High	Yes	Yes	0.55	Yes	Yes	Yes	Yes
ADM	High	No	Yes	0.55	No	Yes	Yes	Yes
AF	High	Yes	Yes	0.55	Yes	Yes	Yes	Yes
AI	High	Yes	No	0.55	Yes	Yes	Yes	Yes
AN	High	No	Yes	0.55	No	Yes	Yes	Yes
ATM	High	No	No	0.55	No	Yes	Yes	Yes

All of the compounds examined exhibited high GI absorption values and passed the 30% criterion, indicating that these newly developed compounds have high human intestine absorption capabilities. All the tested compounds showed moderate water solubility. Out of 11, compounds ACN, AN, ADM and ATM were non-permeant of BBB and ACF, AA, AC, ADC, ADF, AF and AI were the permeant of BBB. Except ACN, ADC, AI and ATM all tested compounds served as Pgp substrate. Also all the tested newly designed indazole scaffolds were observed to inhibit the CYP isoforms except CYP1A2. ACN, ADC, ADM, AN and ATM were found to be non-inhibitors of CYP1A2 and compound ACF, AA, AC, ACF, AF and AI observed to inhibit the CYP1A2. The predicted ADME properties of these newly designed compounds are represented in Table-5.

Conclusion

The molecular docking simulation carried out on indazole based newly designed compounds as VEGFR-2 and InhA inhibitors. In this study, compounds AA (-7.72 kcal/mol) and AF (-7.54 kcal/mol) has highest binding affinity when docked with 4AGD and compounds ADC (-8.30 kcal/mol), ACN (-7.76 kcal/mol) and AI (-7.62 kcal/mol) showed highest binding energy when docked with 2AQK. A significant binding affinity score was found in the majority of newly designed compounds. Drug-likeness and ADME prediction suggest that these compounds are orally bioavailable with good absorption, low toxicity level, and permeable properties and follow Lipinski's Rule of Five, except compound AI passes with one violation. Furthermore, these indazole scaffolds were discovered to have good synthetic accessibility (< 5) indicating that they are easy to synthesize in the lab. The results observed in the present study demonstrated that after further refinement, the newly designed indazole based compounds could be the potential drug of choice for the treatment of non-small cell lung cancer as well as mycobacterium tuberculosis.

ACKNOWLEDGEMENTS

The authors are thankful to the Management of Dr. Vishwanath Karad MIT-World Peace University, Pune, India for the support. The authors are also grateful to DST-SERB for the financial support of this research.

CONFLICT OF INTEREST

The authors declare that there is no conflict of interests regarding the publication of this article.

REFERENCES

1. H. Sung, J. Ferlay, R.L. Siegel, M. Laversanne, I. Soerjomataram, A. Jemal and F. Bray, *CA Cancer J. Clin.*, **71**, 209 (2021); https://doi.org/10.3322/caac.21660
2. Y.Y. Ching, C.H.Y. James and Y.P. Chyr, *Annu. Rev. Med.*, **71**, 117 (2020); https://doi.org/10.1146/annurev-med-051718-013524

3. D.J. Hicklin and L.M. Ellis, *J. Clin. Oncol.*, **23**, 1011 (2005); https://doi.org/10.1200/JCO.2005.06.081
4. R.D. Hall, T.M. Le, D.E. Haggstrom and R.D. Gentzler, *Transl. Lung Cancer Res.*, **4**, 515 (2015); https://doi.org/10.3978/j.issn.2218-6751.2015.06.09
5. R. Roskoski Jr., *Biochem. Biophys. Res. Commun.*, **375**, 287 (2008); https://doi.org/10.1016/j.bbrc.2008.07.121
6. J. Subramanian, D. Morgensztern and R. Govindan, *Clin. Lung Cancer*, **11**, 311 (2010); https://doi.org/10.3816/CLC.2010.n.039
7. J. Zhang, P.L. Yang and N.S. Gray, *Nat. Rev. Cancer*, **9**, 28 (2009); https://doi.org/10.1038/nrc2559
8. P. Wu, T.E. Nielsen and M.H. Clausen, *Trends Pharmacol. Sci.*, **36**, 422 (2015); https://doi.org/10.1016/j.tips.2015.04.005
9. H. Polena, F. Boudou, S. Tilleul, N. Dubois-Colas, C. Lecointe, P. Charles, N. Rakotosamimanana, M. Pelizzola, V. Raharimanga, J.-L. Herrmann, S.F. Andriamandimby, P. Ricciardi-Castagnoli, V. Rasolofo, B. Gicquel and L. Tailleux, *Sci. Rep.*, **6**, 33162 (2016); https://doi.org/10.1038/srep33162
10. A. Spagnuolo, G. Palazzolo, C. Sementa and C. Gridelli, *Expert Opin. Pharmacother.*, **21**, 491 (2020); https://doi.org/10.1080/14656566.2020.1713092
11. https://apps.who.int/iris/bitstream/handle/10665/336069/9789240013131eng.pdf
12. N.M.Y. Elsayed, R.A.T. Serya, M.F. Tolba, M. Ahmed, K. Barakat, D.A. Abou El Ella and K.A.M. Abouzid, *Bioorg. Chem.*, **82**, 340 (2019); https://doi.org/10.1016/j.bioorg.2018.10.071
13. N. Tandon, V. Luxami, D. Kant, R. Tandon and K. Paul, *RSC Adv.*, **11**, 25228 (2021); https://doi.org/10.1039/D1RA03979B
14. V.T. Angelova, T. Pencheva, N. Vassilev, R. Simeonova, G. Momekov and V. Valcheva, *Med. Chem. Res.*, **28**, 485 (2019); https://doi.org/10.1007/s00044-019-02293-w
15. M. Datta, L.E. Via, W.S. Kamoun, C. Liu, W. Chen, G. Seano, D.M. Weiner, D. Schimel, K. England, J.D. Martin, X. Gao, L. Xu, C.E. Barry 3rd and R.K. Jain, *Proc. Natl. Acad. Sci. USA*, **112**, 1827 (2015); https://doi.org/10.1073/pnas.1424563112
16. N.M. O'Boyle, M. Banck, C.A. James, C. Morley, T. Vandermeersch and G.R. Hutchison, *J. Cheminform.*, **3**, 33 (2011); https://doi.org/10.1186/1758-2946-3-33
17. E.F. Pettersen, T.D. Goddard, C.C. Huang, G.S. Couch, D.M. Greenblatt, E.C. Meng and T.E. Ferrin, *J. Comput. Chem.*, **25**, 1605 (2004); https://doi.org/10.1002/jcc.20084
18. S. Forli, R. Huey, M.E. Pique, M.F. Sanner, D.S. Goodsell and A.J. Olson, *Nat. Protoc.*, **11**, 905 (2016); https://doi.org/10.1038/nprot.2016.051
19. L.G. Ferreira, R.S. Dos Santos, G. Oliva and A.D. Andricopulo, *Molecules*, **20**, 13384 (2015); https://doi.org/10.3390/molecules200713384
20. M. McTigue, B.W. Murray, J.H. Chen, Y.-L. Deng, J. Solowiej and R.S. Kania, *Proc. Natl. Acad. Sci. USA*, **109**, 18281 (2012); https://doi.org/10.1073/pnas.1207759109
21. J.S. Oliveira, J.H. Pereira, F. Canduri, N.C. Rodrigues, O.N. de Souza, W.F. de Azevedo, L.A. Basso and D.S. Santos, *J. Mol. Biol.,* **359**, 646 (2006); https://doi.org/10.1016/j.jmb.2006.03.055
22. C.A. Lipinski, F. Lombardo, B.W. Dominy and P.J. Feeney, *Adv. Drug Deliv. Rev.*, **46**, 3 (2001); https://doi.org/10.1016/S0169-409X(00)00129-0
23. A. Daina, O. Michielin and V. Zoete, *Sci. Rep.*, **7**, 42717 (2017); https://doi.org/10.1038/srep42717
24. P. Ertl and A. Schuffenhauer, *J. Cheminform.*, **1**, 8 (2009); https://doi.org/10.1186/1758-2946-1-8
25. M.T. Ibrahim, A. Uzairu, S. Uba and G.A. Shallangwa, *Future J. Pharm. Sci.*, **6**, 55 (2020); https://doi.org/10.1186/s43094-020-00074-6
26. P. Ertl, B. Rohde and P. Selzer, *J. Med. Chem.*, **43**, 3714 (2000); https://doi.org/10.1021/jm000942e
27. A.R. Chabukswar, B.S. Kuchekar, P.D. Lokhande, M. Tryambake, B. Pagare, V. Kadam, S. Jagdale and V. Chabukswar, *Curr. Bioact. Compd.*, **9**, 263 (2013); https://doi.org/10.2174/15734072099991312310955550